

# A new method for determining lumbar spine motion using Bayesian belief network

Heather Ting Ma · Zhengyi Yang · James F. Griffith ·  
Ping Chung Leung · Raymond Y. W. Lee

Received: 21 June 2007 / Accepted: 5 February 2008 / Published online: 23 February 2008  
© International Federation for Medical and Biological Engineering 2008

**Abstract** A Bayesian network dynamic model was developed to determine the kinematics of the intervertebral joints of the lumbar spine. Radiographic images in flexion and extension postures were used as input data for modeling, together with movement information from the skin surface using an electromagnetic motion tracking system. Intervertebral joint movements were then estimated by the graphic network. The validity of the model was tested by comparing the predicted position of the vertebrae in the neutral position with those obtained from the radiographic image in the neutral posture. The correlation between the measured and predicted movements was 0.99 ( $p < 0.01$ ) with a mean error of less than  $1.5^\circ$ . The movement sequence of the various vertebrae was examined based on the model output, and wide variations in the kinematic patterns were observed. The technique is non-invasive and

has potential to be used clinically to measure the kinematics of lumbar intervertebral movement.

**Keywords** Intervertebral kinematics · Bayesian belief networks · Lumbar spine motion · Dynamic modeling · Spine biomechanics

## 1 Introduction

Knowledge of patterns of intervertebral movement of the lumbar spine is clinically useful in the assessment and rehabilitation of spinal disorders [4, 10]. Biomechanical modeling also requires accurate kinematic information as model input data. Nevertheless, measurement of intervertebral movements is technically challenging as the spine is relatively inaccessible and the nature of spinal movement is complex.

Radiographic, electro-optical, electromagnetic and miniature inertial sensing systems have been used in the measurement of lumbar spine motion with some success [2, 3, 6, 18, 19–21, 28, 29, 35]. Surface measurements using optical markers or sensing devices are subjected to considerable error due to interposition of tissue between the spine and the surface markers. Recently, Morl and Blickhan [24] had examined the correlation between the motions of external skin markers and the underlying vertebrae using open magnetic resonance imaging. Although moderate to strong correlation was observed, the measurement errors were found to be high. Surface measurement techniques are only accurate for determining the movement of spine regions as opposed to discriminating the contribution of individual intervertebral joints. Surface measurements that yield accurate intervertebral movement data would require the insertion of pins into the spinous processes [10, 11], but this method has low acceptability for patients.

---

This work was supported by the Hong Kong Research Grant Council (Competitive Earmarked Research Grant CERG CUHK5251/04E).

---

H. T. Ma · J. F. Griffith  
Department of Diagnostic Radiology and Organ Imaging,  
Prince of Wales Hospital, The Chinese University of Hong  
Kong, Shatin, Hong Kong

Z. Yang  
Centre for Magnetic Resonance, University of Queensland,  
Brisbane, QLD, Australia

P. C. Leung  
Department of Orthopaedics and Traumatology, Prince of Wales  
Hospital, Chinese University of Hong Kong, Shatin, Hong Kong

R. Y. W. Lee (✉)  
Clinical Research Centre for Health Professions,  
University of Brighton, Aldro Building, 49 Darley Road,  
Eastbourne, East Sussex BN20 7UR, UK  
e-mail: r.lee@brighton.ac.uk

Only radiographic techniques are able to determine movement of the vertebrae with acceptable accuracy in vivo [28]. Lee and Evans [20] reported that the mean error in determining intervertebral joint motion in the sagittal plane was about  $1.0^\circ$ . However, radiographic techniques such as the videofluoroscopy [27, 38] and cineradiography [17, 35], are complicated, and do involve ionizing radiation.

Sun et al. [34] developed an inverse kinematic model for determining intervertebral motion of the lumbar spine during flexion. The lumbar spine was modeled as an open-ended, kinematic chain of five links, which represented the five vertebrae (L1–L5). An optimization equation with physiological constraints was employed to determine intervertebral joint configuration. The method was found to be very accurate with a high degree of agreement between the predicted movement and the actual movement as determined by radiographic images ( $r = 0.83$ – $0.97$ ). The mean error of prediction (mean difference between radiographic measurement and predicted value) was less than  $1.6^\circ$ . Although this was considered to be accurate, the technique of Sun et al. was able to predict intervertebral displacement in a static neutral or flexed position only. Therefore, we still need a noninvasive and reliable method to study time history of intervertebral joint motions.

A Bayesian belief network is a mathematical model that represents a set of variables and their probabilistic dependencies. It is a graphical model where variables are represented by nodes on a graph, and the arcs joining these nodes encode conditional dependencies between the variables [7, 9, 16]. Such models have recently been employed to solve problems related to the tracking of motions of objects [31, 37], where the target variables (motions of objects) were unknown and might be probabilistically associated with observations or variables that could be measured experimentally. Bayesian network is used to update the state of a set of variables when observations are made. This process of computing the posterior distribution of variable-given evidence is called probabilistic inference, which is implemented by belief propagation algorithms using the Bayes' rule [7, 8, 23, 39]. In this study, we attempted to estimate the intervertebral motions of lumbar spine using observations or cues obtained from motion sensors attached to the skin. Bayesian belief network was employed to describe the probabilistic dependencies between vertebral motions and skin-mounted sensor information and to estimate the intervertebral movements through probabilistic inference.

The purpose of this study was to investigate the feasibility of using a Bayesian belief network model to determine the intervertebral motion of the lumbar spine and to study the motion sequence patterns of the intervertebral joints using the data estimated by the model.

## 2 Methods

This study was carried out on healthy subjects who performed flexion and extension motions of the spine. Radiographic images were obtained statically in three spine postures—flexion, extension and neutral. The flexion and extension images were used as input data for modeling, together with movement information derived from the skin surface using an electromagnetic motion tracking system. The intervertebral joint motions of the spine were then computed. The validity of the model was tested by comparing the predicted position of the vertebrae in the neutral position with those obtained from the radiographic image in the neutral posture. In addition, the timing and sequence of movements of the various intervertebral joints was assessed based on the data estimated by the proposed model.

### 2.1 Subject

Seventeen healthy volunteers (4 males, 17 females, age  $71.8 \pm 3.3$  years, body height =  $156.1 \pm 8.9$  cm, body weight =  $59.0 \pm 11.3$  kg, body mass index =  $24.1 \pm 3.6$ ) were recruited. All subjects had no history of back pain or symptoms attributable to the spine that required medical attention or treatment. Subjects were excluded if there was vertebral body collapse, metastases, spondylolisthesis, spondylolysis, rheumatological disease, or surgery to the lumbar spine. Measurements obtained were part of a health assessment at the Jockey Club Centre for Osteoporosis Care and Control, The Chinese University of Hong Kong [14, 15]. Dual X-ray densitometer (Hologic, Waltham, MA, USA) was used to measure the bone mineral density (BMD) at the lumbar spine. All subjects had normal bone density.

### 2.2 Instrument

An electromagnetic motion tracking system (Fastrak<sup>®</sup>, Polhemus, 40 Hercules Dr, Colchester, Vermont, USA) was used to obtain skin displacement information related to movement of the lumbar spine. This consisted of a source of electromagnetic waves and four miniature motion sensors (Polhemus RX1-D,  $0.9 \text{ mm} \times 0.9 \text{ mm} \times 0.9 \text{ mm}$ ; 20 g). The source was placed in fixed position within one metre of the subject. The four sensors were attached to the skin. The tips of the spinous processes of the first lumbar (L1) and first sacral (S1) vertebrae were identified by palpation. Two sensors were placed over these spinous processes. The other two sensors were evenly distributed between L1 and S1. A previous study demonstrated that the electromagnetic sensors had an angular accuracy of  $\pm 0.2^\circ$  [29]. A software program [17], able to perform fast serial

communication with 120 Hz data update rate, i.e., 30 Hz per sensor sampling rate, was used to acquire and display the data in real time.

### 2.3 Radiograph measurements

Lateral radiographs (Philips M50 CP-H X-ray machine) were obtained for each subject with the sensors attached to the back. Each subject was asked to stand upright with the pelvis rigidly fixed to a frame and the left side of the body facing the film. Lateral images of the lumbar spine (L1–S1) were acquired by a conventional radiographic system in three positions: neutral upright, full flexion, and full extension. In order to accurately define the sensors' location on the radiographic image, two radio-opaque lead markers were fixed on each sensor as shown in Fig. 1. A radio-opaque ruler was also attached to the subject's back in the sagittal plane so that magnification of the vertebrae could be determined.

The coordinates of the vertebral bodies, the tips of the spinous processes, and the lead markers of the sensors were recorded. The L1–L5 vertebral bodies were fitted with quadrangles on each image, as shown in Fig. 1, the corners of the quadrangle representing landmarks for defining the position and orientation of the vertebra. In the case of the sacrum, the posterosuperior and anterosuperior corners of the sacrum were used as landmarks.

In order to validate the prediction of the model, intervertebral joint angles were determined based on the

radiographic images of the vertebral bodies, and compared with those predicted by the model. The sagittal angles of the intervertebral joints were computed from the coordinates of the corners of the two adjoining intervertebral bodies, and the mean error of this measurement was found to be 1.0° [20].

### 2.4 The Bayesian belief network model

In this study, the purpose of modeling was to estimate the intervertebral motions of the lumbar spine using knowledge of the sensor trajectory and the spatial relationship between sensors and the vertebrae as obtained in the flexion and extension radiographic images. Bayesian network was employed to describe the probabilistic dependencies between element nodes and the observations, which represented the variables of interest and the measurable data, respectively. Specifically, the element nodes were the coordinates of two corners (N2 and N3, in Fig. 1) of the vertebral bodies, and the observations were the positions of the skin-mounted Fastrak sensors. Arcs within the networks represented associations among the variables and observations, as shown in Fig. 2. For the model construction, the initial and final spatial relationships between the vertebrae and sensors were defined by the flexion and extension radiographic images. The positions of the vertebrae or the element nodes during the movement from flexion to extension were estimated by the Bayesian network model based on the observations that is, the information obtained from the skin-mounted sensors. Belief propagation

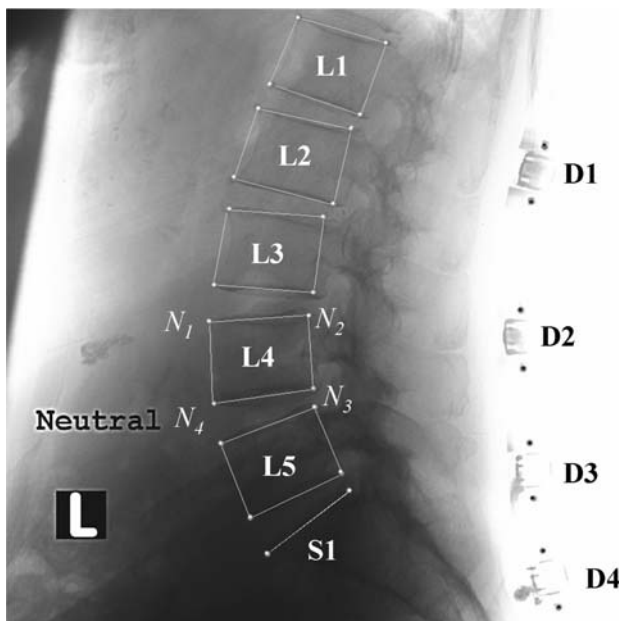


**Fig. 1** Radiographic image showing the reference points for the vertebrae (the white nodes, N<sub>1</sub>–N<sub>4</sub> are illustrated for L4) and the four sensors of the Fastrak system (D1–D4)

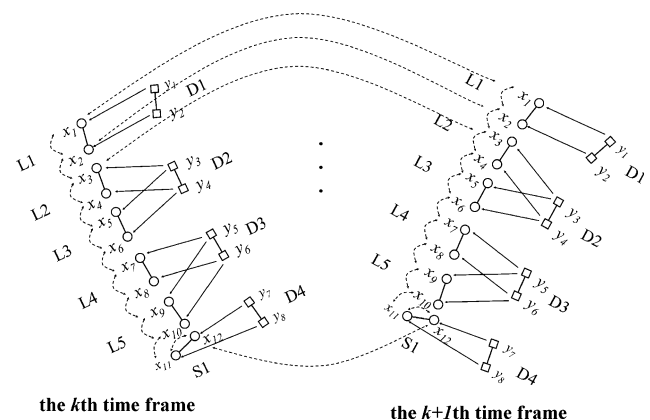


**Fig. 2** The Bayesian network model illustrating the dynamic movement from the kth time frame to the k + 1th time frame. The open circles and open squares represent the element nodes (vertebral position, the x nodes) and observations (sensor position, the y nodes), respectively. Arcs represent the association among element nodes and observations. For simplicity, not all the associations are shown. Thus, the model represents the dynamic process with a Bayesian network, which contains l time frames (only two time frames are shown here) with the same basic local sub-structure. In total, there are l × 12x nodes and l × 8y nodes in the model

algorithms were employed to implement Bayes' probabilistic inference for estimation task.

As a graphical model, Bayesian belief network is a static structure carrying no timing information. In order to model the kinematics of the flexion–extension movement, the Fastrak data in the time domain were projected onto the space domain by transforming the time sequence into space sequence. Therefore, the graphical model included all time frames each of which had a basic structure as illustrated in Fig. 1. The network structure for any two successive time frames is shown in Fig. 2, where  $x$  and  $y$  represent the element node (“circle” in Fig. 2) and observation (“square” in Fig. 2), respectively. The nodes in the network obey the following principles:

1. Among different time frames—each  $x$  node of the  $k$ th time frame is associated with the  $k-1$ th and  $k+1$ th time frame.
2. Within the same time frame—there were probabilistic dependencies between the vertebrae L1–S1 and sensors D1–D4.
3. Associations among  $x$  nodes within the same time frame.
  - (1)  $x_i$  was associated with  $x_{i-1}$  and  $x_{i+1}$ . It was considered that the position of a vertebra was directly influenced by its neighbors.
  - (2)  $x_{12}$  was associated with any other nodes ( $x_1-x_{11}$ ). The local coordinate system was fixed to the sacrum so that it the lumbar vertebrae move with respect to the sacrum.

In Fig. 2, arcs are used to illustrate the main associations among the various nodes and observations. The sensor information is obtained by actual measurement, and therefore probabilistic inference is made in single direction from observation to element node. However, the probabilistic associations between the element nodes are dual directional.

*Belief propagation* algorithm was employed to predict the values of  $x$ -nodes (coordinates of the vertebral body corners) based on the topology of the network model. In brief, the algorithm was implemented as follows.  $\text{Bel}^{(n)}(x_i)$  and  $m_{j \rightarrow i}^{(n)}(x_i)$  represent the *Belief* of the  $i$ th node and the *Message* from the  $j$ th node to the  $i$ th node at the  $n$ th state, respectively.

- (1) Initialization: the initial values of  $\text{Bel}^{(0)}(x_i)$  and  $m_{j \rightarrow i}^{(0)}(x_i)$  are set as zero mean Gaussian distribution with large covariance. Previous research showed that the outline or shape of the vertebrae followed a Gaussian distribution [32].
- (2) Updating for each  $x$  node by calculating the *Belief*

$$\text{Bel}^{(n)}(x_i) = \phi_i(x_i, y_i) \prod_{j \in \Gamma(i)} m_{j \rightarrow i}^{(n)}(x_i) \quad (1)$$

where  $\phi_j(x_j, y_j)$  is the *likelihood* between  $x_j$  node and its observation represented by  $y_j$  node;  $\prod_{j \in \Gamma(i)} m_{j \rightarrow i}^{(n)}(x_i)$  is the prior of  $x_i$  at the  $n$ th state;  $\Gamma(i)$  is the *neighborhood* of node  $i$ ; and  $m_{j \rightarrow i}^{(n)}(x_i)$  is the *message* from node  $j$  to node  $i$  at the  $n$ th state, where  $j \in \Gamma(i)$ .

The association between the variable ( $x$  node) and its observation ( $y$  node) is modeled using coordinate transformation

$$Y = R * X + T \quad (2)$$

where  $X$  and  $Y$  are vectors representing coordinates of any two associated nodes,  $R$  is the rotational matrix, and  $T$  is the translation. Accordingly, the compatibility function  $\phi_j(x_j, y_j)$  in Eq. (1) was defined by a Gaussian distribution of variable  $y_j - R_i^* x_j - t_i$  with zero mean.

The calculation of  $m_{j \rightarrow i}^{(n)}(x_i)$  in Eq. (1) is achieved by two steps:

- (i) Message product at the  $n$ th iteration: multiply incoming messages with the local observation to form a statistical distribution over  $x_j$ .

$$M_j^{(n)}(x_j) = \phi_j(x_j, y_j) \prod_{k \in \Gamma(j)} m_{k \rightarrow j}^{(n-1)}(x_j) \quad (3)$$

where  $\phi_j(x_j, y_j)$  is the *likelihood* between  $x_j$  node and its observation  $y_j$ ;  $\Gamma(j)$  is the *neighborhood* of node  $j$ ; and  $m_{k \rightarrow j}^{(n)}(x_j)$  is the *message* from node  $k$  to node  $j$  at the  $n$ th state, where  $k \in \Gamma(j)$ .

- (ii) Message propagation at the  $n$ th state: transform distribution from  $x_j$  node to  $x_i$  node using the pairwise interaction compatibility function  $\psi_{ji}(x_j, x_i)$ .

$$m_{j \rightarrow i}^{(n)}(x_i) = \int \psi_{ji}(x_j, x_i) M_j^{(n)}(x_j) dx_j \quad (4)$$

At the  $n$ th state, by integrating over  $x_j$ , all the  $j$ th node prior knowledge about  $i$ th node is summarized and transformed to the  $i$ th node. Similar to  $\phi_j(x_j, y_j)$ , the pairwise interaction compatibility function  $\psi_{ji}(x_j, x_i)$  in Eq. (4) describes the association between  $x_i$  and  $x_j$  which is a coordinate transformation as shown in Eq. (2). Therefore,  $\psi_{ji}(x_j, x_i)$  is defined in the same manner as  $\phi_j(x_j, y_j)$ , i.e.,  $x_i - R_{ji}^* x_j - t_{ji}$ , where  $R_{ji}$  and  $t_{ji}$  are the rotation matrix and displacement from the  $j$ th node to the  $i$ th node. The initial and final values of rotation matrix ( $R$ ) and the displacement ( $T$ ) in  $\psi_{ji}(x_j, x_i)$  are set, respectively, by the position information of  $x_i$  and  $x_j$  extracted from the two boundary frames in the model.

Finally, Eq. (4) is substituted into Eq. (1), updating the distribution of  $x_i$  at the  $n$ th state, i.e.,  $\text{Bel}^{(n)}(x_i)$ .

- (3) Iteratively calculating the *Belief* for all the variable nodes until the termination condition  $(\text{Bel}^{(n)}(x_i) - \text{Bel}^{(n-1)}(x_i) < \varepsilon, \varepsilon = 10^{-5})$  was satisfied, allowing the convergence of the ultimate state value.
- (4) The mean values of  $\text{Bel}^{(n)}(x_i)$  in the last state were taken as the ultimate estimation of the *i*th node, i.e., the coordinates of vertebral landmarks. The sagittal angles of the intervertebral joints were then computed from the ultimate estimates of the coordinates of the corners of the two adjoining intervertebral bodies [20].

### 2.5 Movement sequence patterns of the lumbar spine

Using the data predicted by the model, the movement sequencing of the intervertebral joints of the lumbar spine was determined for four movements—extension-neutral, neutral-flexion, flexion-neutral, and neutral-extension. In order to provide uniform data length for all movement-time curves, data was normalized with respect to time using the spline function, and expressed as percentage of the total time. An intervertebral joint was considered to start moving when the change in joint angle became greater than 1°. Movement sequence was determined from the order of movements using the proposal of Gatton and Percy [5]. Five categories of movement sequence were defined—“all together” (where all joints started movement simultaneously), “bottom up” (when the bottom of the lumbar spine L5/S1 was first to move, and the top T12/L1 last to move), “middle first” (when the middle joints, i.e., either L2/3 or L3/4, moved first), “top down” (when the T12/L1 joint moved first and the L5/S1 joint moved last), and “other” (not fitting anyone of the above categories).

## 3 Results

### 3.1 Validation of model

Based on the boundary conditions provided by the radiographic images at the end of flexion and extension, the Bayesian belief network model predicted the coordinates of the vertebral landmark-given observations (coordinates of radio-opaque markers on the sensors). Figure 3 is an example of the intervertebral joint motion of the lumbar spine of one subject that was predicted by the model. For the purpose of validation, the intervertebral angles from the radiographic image in the neutral posture were compared with those calculated from the estimation from the model. The correlation coefficient between the estimated movements and the actual movements recorded on radiographs was found to be 0.99 ( $p < 0.01$ ), indicating a very high

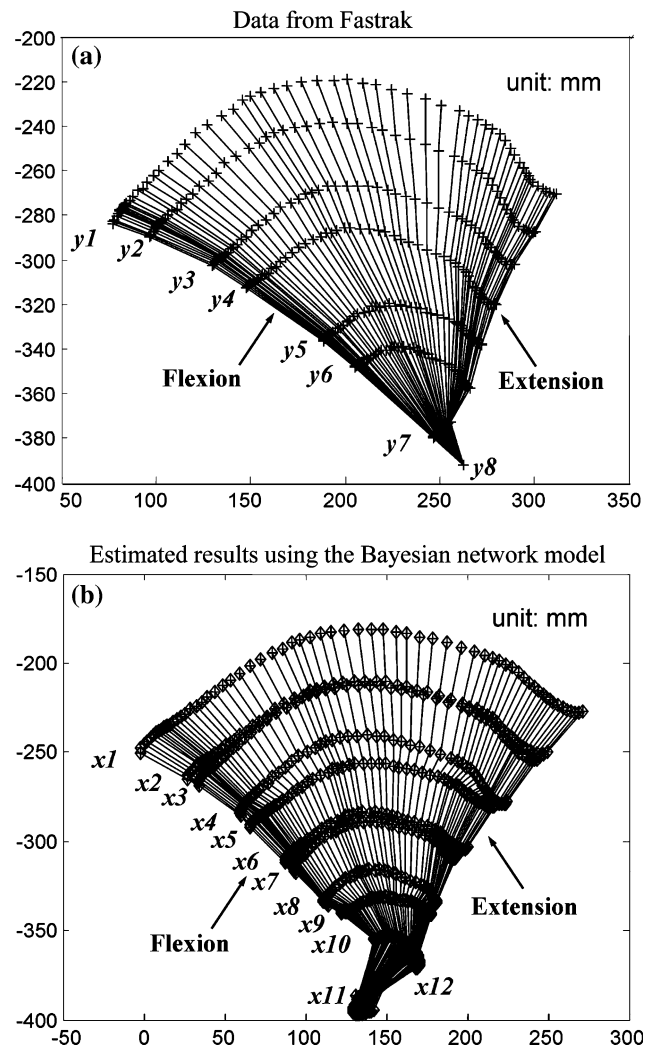


**Fig. 3** The dynamic movement of the lumbar vertebrae estimated by the Bayesian network model using data from the Fastrak sensors. The final positions of flexion and extension are shown.  $x_1$ – $x_{12}$  and  $y_1$ – $y_8$ , which are the lumbar vertebra and the skin-mounted sensors, respectively

degree of agreement. Error was defined as the difference between measured and predicted values. The magnitude of error of the various intervertebral joints is shown in Fig. 4. The overall mean error was found to be  $-1.45^\circ \pm 3.34^\circ$ , where the L2/3 and L5/S1 joints had the least and largest mean errors, respectively. The error was considered to be small, and the model accurate enough for predicting intervertebral joint motion.

### 3.2 Movement sequence patterns

There were wide variations in the movement sequences of the intervertebral joints among subjects. Table 1 shows the frequency of occurrence of each movement pattern. Most subjects exhibited patterns, which were not classifiable and



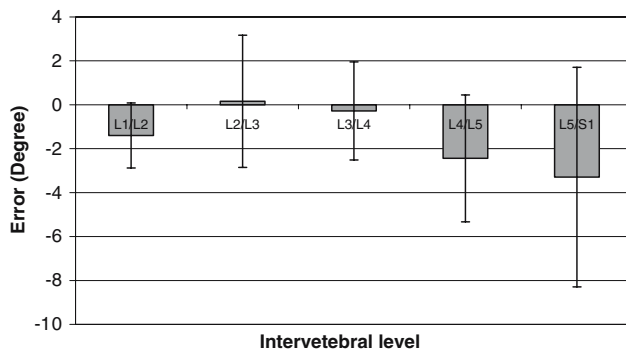


**Fig. 4** Prediction error for the intervertebral angles (unit: degree)

belonged to the category “others”. The most frequently observed sequence was the “bottom-up” pattern, and no subject exhibited the “top-down” pattern. It was noted that for subjects classified as the same sequence pattern, the rate of change of intervertebral angles (velocities) varied from subject to subject. Interestingly, it was also observed that some individual joints extended during flexion motion and vice versa.

#### 4 Discussions

This study was the first attempt to determine the kinematics and movement patterns of the intervertebral joints using the Bayesian belief network model, a model, which is commonly used in artificial intelligence [13]. The degree of correlation between the measured and predicted movements was excellent with a mean error of less than  $1.5^\circ$ . Some previous studies [20, 34] had reported accuracy of similar magnitude, but they analyzed only intervertebral displacement information only in the static posture. The current model has many other potential benefits. For instance, it is easier to operate and computationally less complex when compared to the inverse kinematic model proposed by Sun et al. [34]. Unlike previous models, the Bayesian model makes no assumption about the geometry and structure of the kinematic chain, and is therefore highly robust for predicting spinal motions.

Measurements of spinal motions using skin-mounted sensors are subjected to considerable error due to soft tissue deformation between the spine and the sensors. The

sensor displacements may not reliably represent the actual spinal motions. Due to the soft tissue deformation, the spatial association between the vertebrae and the sensors are constantly changing. It would be impossible to establish this association using traditional statistical methods such as correlation or regression because the soft tissue deformation is rather unpredictable. However, the present model solves this problem by estimating the spatial association between the vertebrae and the sensor through probabilistic inference using the belief propagation algorithm. This allows spinal motions to be successfully determined using surface information, as demonstrated by the small error observed in this study.

Table 1 shows that the L5/S1 joint was subjected to a larger error compared to the other intervertebral joints. This is mainly because one landmark on the S1 vertebra is remote to the sensor site (in Fig. 1, 2). In the model construction, two upper corners of the sacrum were chosen as landmarks to define the bone position. One of the element nodes for S1,  $x_{11}$  (Fig. 2), was further away from the vertebra when compared to the other element nodes. This increased node distance may have accounted for the larger prediction error observed in the L5/S1 joint. Equations (1)–(4) of the model show that node distance is an essential factor in the algorithms for belief propagation. A smaller distance would result in a more reliable relationship between the element node and the observation. This problem can be minimized in future by choosing another bony landmark such as the S2 spinous process.

This study clearly shows that there is wide variation in the way that the lumbar spine moves between subjects. The variability in the motion sequence patterns is illustrated in Table 1. This is largely because the human spine has redundant degree of freedom, giving great flexibility in the performance of a movement. For instance, spinal flexion can be accomplished with infinite configurations of the intervertebral joints. Previous studies on lumbar spine kinematics assumed certain patterns in movement sequence of the lumbar spine. For instance, Kanayama et al. [12] suggested that during forward flexion the spine moves from the top first, though this was not observed in this study. McGill [25] assumed that all the intervertebral joints moved at the same time in his model, but in this study, only about 4% of examinations showed an “all together”

**Table 1** Movement sequence patterns of the intervertebral joints of the lumbar spine

	Extension → Neutral	Neutral → Flexion	Flexion → Neutral	Neutral → Extension
All together	2	1	0	0
Bottom up	6	5	5	3
Middle first	3	4	0	4
Top down	0	0	0	0
Others	6	7	12	10

pattern. Our study supports the findings of Gattton and Pearcy [5], who reported that different spines exhibit different movement sequences. Both our study and this earlier work showed that the “bottom-up” pattern was the most common pattern. However, our study may provide more reliable data because our work was based on the best estimates of intervertebral motions using probabilistic inference. The observation of Gattton and Pearcy was only based on information obtained from skin-mounted sensors and they did not estimate the underlying intervertebral motions.

The most interesting finding in this study was that some intervertebral joints move in a direction opposite to the direction of bending of the lumbar spine. That is, some joints exhibited extension during flexion of the spine and vice versa. Such aberrant motion has also been reported by previous studies [5, 22, 26, 28, 30, 33, 36]. The movement patterns of the spine are often oversimplified in many textbooks, and this study had provided a detailed description of subject variability in the spinal motion pattern. However, our sample size is small, and a larger study will be required to fully document the various patterns. For this purpose, our study does provide a valid and accurate model, which allows an easier assessment of spinal motion. The clinical implications of the aberrant motions are still unclear, and further studies will be required to address this issue.

Future biomechanical studies will benefit from the dynamic model developed in this study. The actual intervertebral rotations can be predicted by the model, and no assumptions have to be made regarding the movement pattern. The relationship among the various segments did not have to be assumed to be constant throughout the movement. The accuracy of the biomechanical model is thus tremendously improved. This will allow us to study how different kinematic patterns in different individuals produce different loading patterns in the spine.

Knowledge of the kinematic patterns of the spine may also be useful in the clinical assessment of spinal disorders such as back pain, spondylolysis or spondylolisthesis. A major attraction of the model is that it provides kinematic data and allows us to determine the higher derivatives of motions such as velocities and accelerations. Previous research showed a significant relationship between back pain and intervertebral motion [1]. The association between pain and higher movement derivatives is still unclear. This can be explored using the present model.

It should be pointed out that the present study was conducted in a group of elderly subjects. It is likely that the Bayesian belief network model could also be employed in younger subjects with similar accuracy. However, the kinematic and movement sequence pattern observed in this study may not be generalized to the younger age group, and

this will need to be clarified in future studies. It would also be interesting to study how activity level and quality of life may influence the kinematic patterns among the elderly subjects.

## 5 Conclusion

This is the first study, which employs a Bayesian belief network model to study the kinematic pattern of the intervertebral movement of the lumbar spine. The developed model is able to estimate the intervertebral angle reliably with a mean error of less than  $1.5^\circ$ . The technique is non-invasive and has the potential to be used clinically to measure kinematics of intervertebral movement. It will also be useful to biomechanical modelling when kinematic data are required as input variables. This study showed a wide variation in the kinematic patterns in the subjects studied. The present model may also be used to study velocity and acceleration of intervertebral joint providing further insight into the kinematics of the lumbar spine.

**Acknowledgments** This work was supported by the Hong Kong Research Grant Council (Competitive Earmarked Research Grant CERG CUHK5251/04E).

## References

1. Abbott J, Fritz J, McCane B, Shultz B, Herbison P, Lyons B, Stefanko G, Walsh R (2006) Lumbar segmental mobility disorders: comparison of two methods of defining abnormal displacement kinematics in a cohort of patients with non-specific mechanical low back pain. *BMC Musculoskelet Disord* 7:45
2. Dvorak J, Panjabi MM, Chang DG, Theiler K, Grob D (1991) Functional radiographic diagnosis of the lumbar spine. Flexion-extension and lateral bending. *Spine* 16:562–571
3. Dumas R, Blanchard B, Carlier R, de Loubresse CG, Le Huec JC, Marty C, Moinard M, Vital JM (2008) A semi-automated method using interpolation and optimisation for the 3D reconstruction of the spine from bi-planar radiography: a precision and accuracy study. *Med Biol Eng Comput* 46:85–92
4. Frymoyer J, Pope M, Wilder D (1990) Segmental instability. In: Weinstein J, Wiesel S (eds) *The lumbar spine*. WB Saunders, Philadelphia, pp. 612–636
5. Gattton ML, Pearcy MJ (1999) Kinematics and movement sequencing during flexion of the lumbar spine. *Clin Biomech* 14:376–383
6. Goodvin C, Park EJ, Huang K, Sakaki K (2006) Development of a real-time three-dimensional spinal motion measurement system for clinical practice. *Med Biol Eng Comput* 44:1061–1075
7. Jensen FV (1996) *An introduction to Bayesian networks*. UCL Press, London
8. Jordan MI, Ghahramani Z, Jaakkola TS, Saul LK (1999) An introduction to variational methods for graphical models. *Mach Learn* 37:183–233
9. Jordan MI (2004) Graphical models. *Stat Sci* 19:140–155
10. Kaigle A, Pope M, Fleming B, Hansson T (1992) A method for the intravital measurement of interspinous kinematics. *J Biomech* 25:451–456

11. Kanayama M, Abumi K, Kaneda K, Tadano S, Ukai T (1996) Phase lag of the intersegmental motion in flexion–extension of the lumbar and lumbosacral spine: an in vivo study. *Spine* 21:1416–1422
12. Kanayama M, Tadano S, Kaneda K, Ukai T, Abumi K, Ito M (1995) A cineradiographic study on the lumbar disc deformation during flexion and extension of the trunk. *Clin Biomech* 10:193–199
13. Korb KB, Nicholson AE (2003) Bayesian artificial intelligence. Chapman & Hall/CRC, Florida
14. Lau MC, Chan YH, Chan M, Woo J, Griffith J, Chan HL, Leung PC (2000) Vertebral deformity in Chinese men: prevalence, risk factors, bone mineral density, and body composition measurements. *Calcif Tissue Int* 66:47–52
15. Lau MC, Woo J, Chan H, Chan KF, Griffith JF, Chan YH, Leung PC (1998) The health consequences of vertebral deformity in elderly Chinese men and women. *Calcif Tissue Int* 63:1–4
16. Lauritzen SL, Wermuth N (1989) Graphical models for associations between variables, some of which are qualitative and some quantitative. *Ann Stat* 17:31–57
17. Lee R (2002) Measurement of movements of the lumbar spine. *Physiother Theory Pract* 18:159–164
18. Lee RYW (1995) The biomechanical basis of spinal manual therapy. University of Strathclyde, Glasgow
19. Lee RYW (2001) Kinematics of rotational mobilisation of the lumbar spine. *Clin Biomech* 16:481–488
20. Lee RYW, Evans JH (1997) An in vivo study of the intervertebral movements produced by posteroanterior mobilisation. *Clin Biomech* 12:400–408
21. Lee RYW, Laprade J, Fung EH (2003) A real-time gyroscopic system for three-dimensional measurement of lumbar spine motion. *Med Eng Phys* 25:817–824
22. Lehman GJ (2004) Biomechanical assessments of lumbar spinal function. how low back pain sufferers differ from normals. Implications for outcome measures research. part i: kinematic assessments of lumbar function. *J Manipulative Physiol Ther* 27:57–62
23. MacKay DJC (2003) Exact Marginalization in Graphs. In: MacKay DJC (ed) *Information theory, inference, and learning algorithms*. Cambridge University Press, Cambridge, pp. 334–340
24. Morl F, Blickham R (2006) Three-dimensional relation of skin markers to lumbar vertebrae of healthy subjects in different postures measured by open MRI. *Eur Spine J* 15:742–751
25. McGill SM, Norman RW (1986) Partitioning of the L4–L5 dynamic moment into disc, ligamentous and muscular components during lifting. *Spine* 11:666–678
26. Nattrass CL, Nitschke JE, Disler PB, Chou MJ, Ooi KT (1999) Lumbar spine range of motion as a measure of physical and functional impairment: an investigation of validity. *Clin Rehabil* 13:211–218
27. Okawa A, Shinomiya K, Komori H, Muneta T, Arai Y, Nakai O (1998) Dynamic motion study of the whole lumbar spine by videofluoroscopy. *Spine* 23:1743–1749
28. Percy MJ (1985) Stereo radiography of lumbar spine motion. *Acta Orthop Scand* 56(Suppl 212):1–45
29. Percy MJ, Hindle RJ (1989) New method for the non-invasive three dimensional measurement of human back movement. *Clin Biomech* 4:73–79
30. Selles RW, Wagenaar RC, Smit TH, Wuisman PI (2001) Disorders in trunk rotation during walking in patients with low back pain: a dynamical systems approach. *Clin Biomech* 16:175–181
31. Sigal L, Bhatia S, Roth S, Black MJ, Isard M (2004) Tracking loose-limbed people. In: *The 2004 IEEE computer society conference on computer vision and pattern recognition (CVPR 2004)*, Washington, DC, USA
32. Smyth PP, Taylor CJ, Adams JE (1999) Vertebral shape: automatic measurement with active shape models. *Radiology* 211:571–578
33. Sullivan MS, Shoaf LD, Riddle DL (2000) The relationship of lumbar flexion to disability in patients with low back pain. *Phys Ther* 80:240–250
34. Sun LW, Lee RYW, Lu W, Luk DK (2004) Modelling and simulation of the intervertebral movements of the lumbar spine using an inverse kinematic algorithm. *Med Biol Eng Comput* 42:740–746
35. Takayanagi K, Takahashi K, Yamagata M, Moriya H, Kitahara H, Tamaki T (2001) Using cineradiography for continuous dynamic-motion analysis of the lumbar spine. *Spine* 26:1858–1865
36. Teyhen DS, Flynn TW, Childs JD, Kuklo TR, Rosner MK, Polly DW, Abraham LD (2007) Fluoroscopic video to identify aberrant lumbar motion. *Spine* 32:E220–E229
37. Toyama K, Blake A (2002) Probabilistic tracking with exemplars in a metric space. *Int J Comput Vis* 48:9–19
38. Wong KWN, Luk KDK, Leong JCY, Wong SF, Wong KKY (2006) Continuous dynamic spinal motion analysis. *Spine* 31:414–419
39. Yedidia JS, Freeman WT, Weiss Y (2003) Understanding belief propagation and its generalizations. In: Lakemeyer G, Nebel B (eds) *Exploring artificial intelligence in the new millennium*. Morgan Kaufmann Publishers, San Francisco, pp 239–270